[CANCER RESEARCH 63, 5420–5427, September 1, 2003]

Hemangiosarcomas, Medulloblastomas, and Other Tumors in *Ink4c/p53*-null Mice[1]

Frederique Zindy,[2] Lisa M. Nilsson,[2] Luc Nguyen, Cecile Meunier, Richard J. Smeyne, Jerold E. Rehg, Charles Eberhart, Charles J. Sherr, and Martine F. Roussel[3]

Departments of Genetics and Tumor Cell Biology [F. Z., L. M. N., L. N., C. M., C. J. S., M. F. R.], Developmental Neurobiology [R. J. S.], and Pathology [J. E. R.] and Howard Hughes Medical Institute [C. J. S.], St. Jude Children's Research Hospital, Memphis, Tennessee 38105, and Department of Pathology, Johns Hopkins School of Medicine, Baltimore, Maryland 21205 [C. E.]

ABSTRACT

Ink4 proteins inhibit the enzymatic activities of cyclin D-dependent kinases, thereby governing transcriptional programs that depend on the activities of the retinoblastoma protein and other retinoblastoma family members (p107 and p130). Mice lacking *Ink4c* and *p53* spontaneously develop a broad spectrum of neoplasms, usually presenting with multiple tumors of different histological types and dying of cancer by 6 months of age. Whereas thymic lymphomas or pituitary tumors predominate in mice lacking *p53* or *Ink4c*, respectively, animals lacking both genes develop many vascular tumors and also present with medulloblastomas not observed in the parental strains. Unlike *p53*, loss of the *Arf* tumor suppressor did not contribute to the appearance of vascular or cerebellar tumors. Vascular tumors ranged in severity from angiomas to hemangiosarcomas, some of which could be transplanted into immunocompromised mice. Intriguingly, loss of *Ink4c* but maintenance of at least one *Ink4d* allele was required for formation of medulloblastomas in *p53*-null mice. *In situ* hybridization revealed that, in newborn mice, *Ink4c* is detected in the pia mater and in an adjacent layer of rapidly dividing cells within the cerebellar external granule layer (EGL), whereas *Ink4d* is primarily expressed in Purkinje neurons. Because the pia mater and Purkinje cells sandwich the cerebellar EGL from which medulloblastomas are presumed to arise, Ink4 proteins might function in a cell-autonomous manner in governing neuronal cell cycle exit as well as in a non-cell-autonomous manner in controlling the production of diffusible mitogens and chemokines that influence postnatal development of the cerebellar EGL.

INTRODUCTION

By antagonizing the activities of CDKs,[4] expression of CKIs enforces exit from the cell division cycle and actively maintains cells in a quiescent state. Loss of function of certain CKIs during organismal development can lead to unscheduled proliferation, resulting in organomegally, defects in the execution of certain differentiation programs, and susceptibility to tumor formation later in life (1–4). CKIs belong to two distinct gene families. The Ink4 proteins ($p16^{Ink4a}$, $p15^{Ink4b}$, $p18^{Ink4c}$, and $p19^{Ink4d}$) specifically bind to and inhibit the activity of the CDKs, CDK4 and CDK6 (1, 4). Ink4 polypeptides prevent phosphorylation of proteins of the Rb gene family (including Rb itself, p107, and p130), thereby maintaining them in their active, growth-inhibitory states. In turn, Rb family members suppress the transcription of E2F-responsive genes that normally drive the entry of cells into the DNA synthetic (S) phase of the cell division cycle (5–7). Members of a second family of CKIs, the Cip/Kip proteins ($p21^{Cip1}$, $p27^{Kip1}$, and $p57^{Kip2}$), are potent inhibitors of cyclin E- and A-dependent CDK2 and reinforce the Ink4 proteins in inhibiting S-phase entry and progression (8). Members of both CKI families can complement one another's functions during development, sometimes through co-expression in particular cell types, but also by coordinating the behavior of interacting cell populations in developing organs (2, 3).

CKI proteins are differentially expressed during mouse embryonic development and in adult tissues. Whereas *Ink4a* and *Ink4b* are not normally expressed in embryos or in young animals, *Ink4c* and *Ink4d* are ubiquitously expressed in embryos and in many tissues of adult mice, usually in nonoverlapping patterns (9). Both *Ink4c* and *Ink4d* are expressed in many regions of the developing central nervous system; *Ink4c* seems to be preferentially localized to proliferating neurons as they exit the cell cycle, whereas *Ink4d* is detected mainly in postmitotic neurons (10). Expression of $p19^{Ink4d}$ and $p27^{Kip1}$ is maintained in postmitotic cells of the adult brain, including Purkinje and granule neurons in the adult cerebellum (10). Codeletion of both genes in the mouse allows differentiated neurons in various parts of the brain to undergo inappropriate cell divisions, leading to neuronal apoptosis and, ultimately, to gross neurological dysfunction and death between P14 and P24 (11). This suggests that $p19^{Ink4d}$ and $p27^{Kip1}$ normally collaborate to actively maintain certain neurons in a postmitotic state. In contrast, in the organ of Corti within the inner ear, $p19^{Ink4d}$ alone is required for maintenance of sensory hair cells in a quiescent state, whereas $p27^{Kip1}$ keeps supporting cells from dividing. Loss of *Kip1* leads to the appearance of supernumerary supporting cells, whereas disruption of *Ink4d* induces sensory hair cells to reenter the cell cycle and die, with loss of either CKI leading to deafness (12, 13). Like mice lacking *Kip1* (14–16), animals lacking *Ink4c* exhibit organomegally (17, 18). Both *Kip1*-null and *Ink4c*-null mice develop pituitary adenomas (14–18), whose time of onset is greatly accelerated in animals lacking both genes (17, 19).

Loss of *Ink4d* does not accelerate tumor formation in *Ink4c*-null mice, but males lacking these two CKIs cannot produce viable sperm and are sterile (20). We interbred the *Ink4c/Ink4d*-null mice with animals lacking p53, reasoning that apoptosis in developing male germ cells might be mitigated on a *p53*-null background and lead to testicular tumors. Mice lacking both *Ink4c* and *p53* were highly tumor-prone, and the frequency of germ cell tumors was not increased by codeletion of *Ink4d*. Instead, we detected a high incidence of vascular tumors, as well as medulloblastomas. Studies of *Ink4c* and *Ink4d* expression in the developing cerebellum indicated that *Ink4c* is expressed primarily in cells of the pia mater and, between P5 and P10, in rapidly dividing cells of the EGL that are presumed to give rise to medulloblastoma. In contrast, *Ink4d* expression is restricted to Purkinje neurons. These data suggest that *Ink4* proteins may play both cell-autonomous and non-cell-autonomous roles in tumor formation.

Received 4/14/03; revised 6/5/03; accepted 6/18/03.

The costs of publication of this article were defrayed in part by the payment of page charges. This article must therefore be hereby marked *advertisement* in accordance with 18 U.S.C. Section 1734 solely to indicate this fact.

[1] Supported by NIH Grants CA 71907 (to M. F. R.), R25 CA23944 (to L. N.), Cancer Center Core Grant CA 21765, and by the American Lebanese Syrian Associated Charities of St. Jude Children's Research Hospital. C. E. is the recipient of a Burroughs Wellcome Career Award in the Biomedical Sciences. C. J. S. is an Investigator of the Howard Hughes Medical Institute.

[2] Both of these authors contributed equally to this work.

[3] To whom requests for reprints should be addressed, at St. Jude Children's Research Hospital, Danny Thomas Research Tower, 5006C, Mail stop 350, 332 North Lauderdale, Memphis, TN, 38105. Phone: (901) 495-3481; E-mail: martine.roussel@stjude.org.

[4] The abbreviations used are: CDK, cyclin-dependent kinase; CKI, CDK-inhibitory protein; Rb, retinoblastoma; P, postnatal day; E, embryonic day; EGL, external granule layer; NOD, nonobese diabetic; SCID, severe combined immunodeficient; VEGF-R2, vascular endothelial growth factor receptor 2; GFAP, glial fibrillary acidic protein; PNET, primitive neuroectodermal tumor; DZ, differentiating zone; NE, neuroepithelial zone; GT, germinal trigone; PCP, Purkinje cell precursor; IGL, internal granular layer; GCP, granule cell precursor; Shh, Sonic hedgehog.

MATERIALS AND METHODS

Mouse Colonies. Female mice doubly deficient for *Ink4d* and *Ink4c* (20) were crossed with *p53*-deficient males (Jackson Laboratory, Bar Harbor, ME) to generate mice heterozygous for all three genes. The latter were intercrossed to generate compound genotypes, which were born at the expected Mendelian frequencies. All mice were from a mixed (129SvJ × C57BL/6) genetic background. Genotyping for *p53* (21) or *Ink4c* (18) was performed by PCR. *Ink4d* genotyping by PCR used the following primers: wild-type *Ink4d* alleles were amplified with forward primer 5′-CAAGATGCCTCCGGTACTAG-3′ and reverse primer 5′-AAGCTGACCACGGAGCTATG-3′; and the *Ink4d*-null allele was amplified using forward primer 5′-CACGAGATTTCGATTC-CACC-3′, and the same reverse primer used for the wild-type allele. The animals were maintained in accordance with approved St. Jude Children's Research Hospital guidelines and observed daily for up to 6 months of age.

Tumor and Cell Transplants. EOMA cells [a kind gift from R. Auerbach (University of Wisconsin); Ref. 22] were transplanted by injection of 1×10^6 cells s.c. on each shoulder of NOD/SCID mice. Hemangiosarcomas were transplanted into NOD/SCID mice as described previously (23). Tumor growth was monitored daily.

Histopathology, Immunohistochemistry, and *in Situ* RNA Hybridization. Moribund mice were sacrificed using CO_2 inhalation. Tumors and organs from each animal were systematically collected for pathology and immunohistochemical analyses. Tissues were fixed in 10% neutral-buffered formalin and embedded in paraffin. Tissue sections of 5 μm were stained with H&E for histopathological analysis and characterized by immunohistochemistry (24). Heat-induced epitope retrieval was performed in citrate buffer (pH 6.0) or in target retrieval solution (pH 6.2; DAKO, Carpinteria, CA) as described previously (25). Vascular tumors were stained with antibodies to proteins that characteristically mark endothelial cells: CD31 and CD34 (PharMingen, San Diego, CA); VEGF-R2 (R&D Systems, Minneapolis, MN); and Factor 8 (DAKO). B- and T-cell lymphomas were characterized by staining with antibodies to CD3, CD45R/B220, CD138, terminal deoxynucleotidyl transferase, IgM, and κ light chain as described previously (25). Non-vascular tumors were stained with antibodies to determinants expressed on soft tissue mesenchymal and epithelial cells: desmin, muscle-specific actin, myogenin, smooth muscle actin, cytokeratin wide spectrum, and S-100 (all from DAKO); and cytokeratin AE1/AE3 (Chemicon International, Temecula, CA). Biotinylated second antibodies were from Vector Laboratories (Burlingame, CA) or Santa Cruz Biotechnology (Santa Cruz, CA). Negative controls were prepared by omitting primary antibody and substituting isotype-matched IgGs at equivalent concentrations.

For examination of brain tumors, formalin-fixed, paraffin-embedded mouse brain sections were deparaffinized, and antigen retrieval was performed for 1 min in a pressure cooker with antigen unmasking solution (Vector Laboratories). Endogenous peroxidase activity was quenched with 3% H_2O_2 for 5 min at room temperature. Sections were incubated for 45 min at room temperature with mouse monoclonal antibodies specific for nestin (1:300; BD PharMingen) or synaptophysin (1:100; DAKO) or with rabbit polyclonal antibodies for GFAP (1:1000; DAKO). Primary antibodies were visualized with either mouse or rabbit Vectastain Elite ABC kits (Vector Laboratories) following manufacturer's instructions. *In situ* hybridizations were performed with antisense probes from *Ink4d* and *Ink4c* mouse cDNAs on sections of heads from E11.5 embryos to P5 and on sections of brain from adult mice, as described previously (10).

RESULTS

Mice Lacking *Ink4c* and *p53* Rapidly Develop a Broad Spectrum of Tumors. Disruption of *p53* in the mouse germ line primarily predisposes the animals to thymic lymphomas (~70% incidence), leading to the death of afflicted animals within 6 months of birth (21, 26). Other tumors arising in *p53*-null animals include teratomas and sarcomas of various origins, including hemangiosarcomas at a significant but relatively low incidence (8–23%, depending on genetic background; Ref. 27). The overall incidence of sarcomas (57% penetrance) is increased in $p53^{+/-}$ strains where the wild-type *p53* allele is inactivated in the tumors, but the fraction of hemangiosarcomas is not correspondingly elevated (21). *Ink4c*-null mice, as well as those lacking both *Ink4c* and *Ink4d*, develop pituitary intermediate lobe tumors (75%) and T-cell lymphomas (~10%) late in life, with mean latencies of 12 and 14 months, respectively (17, 18, 20).

Our initial goal was to try to restore male fertility in *Ink4c*/*Ink4d*-null mice by inhibiting p53-dependent apoptosis, so we bred these animals onto a *p53*-null or *Arf*-null background. Mice lacking *p53* and one or two *Ink4c* alleles, regardless of *Ink4d* status, became moribund as early as 2 months of age, and by ~30 weeks, all had succumbed to cancer (Fig. 1). In contrast, when crossed into an *Arf*-null background, mice lacking *Ink4c* did not develop any overt disease by 4 months of age, apart from incipient pituitary tumors. The survival curves (Fig. 1) suggest that animals lacking *p53* and only one copy of *Ink4c* develop tumors more slowly than mice lacking both *Ink4c* alleles, but these apparent differences were not statistically significant, given the sizes of the cohorts studied.

In general, by the time they became ill, animals lacking *p53* and at least one *Ink4c* allele had spontaneously developed multiple tumors, frequently arising from completely different cell types (Table 1). Loss of one or two copies of *Ink4c* together with *p53* did not significantly accelerate the onset of thymic lymphomas (mean latency, 16 weeks) that are associated with *p53* loss alone. Animals lacking both *Ink4c* alleles (or, in one case, only one) developed mid-lobe pituitary adenomas, as expected (17, 18). Mice lacking *p53* and one (~83%) or both (~88%) *Ink4c* alleles also developed endothelial cell hyperplasias and vascular tumors of different degrees of severity, regardless of their *Ink4d* status. A significant number of animals developed brain tumors, most of which were medulloblastomas. Intriguingly, although medulloblastomas appeared in animals lacking one or both *Ink4c* alleles, no such tumors were observed in animals that also lacked both copies of *Ink4d*. Therefore, retention of *Ink4d* appears to facilitate medulloblastoma formation in the *p53*/*Ink4c*-null setting (see below).

Vascular Tumors in Mice Lacking *Ink4c* and *p53*. Vascular tumors in *p53*-null animals lacking one or both *Ink4c* alleles arose at many different sites, including the heart, skeletal muscles, and s.c. tissues and in the omentum. In some cases, necropsy revealed the presence of multiple vascular tumors in addition to the other tumors types summarized in Table 1. A gradient of pathologies was observed ranging from simple endothelial cell hyperplasia and benign angiomas to frank hemangiosarcomas (Fig. 2*A*). Histological staining revealed the presence of highly vascularized tissues with pleomorphic, dense nuclei and visible mitotic figures (Fig. 2*B*). Cells within the tumor masses expressed endothelial markers including CD31 (Fig. 2*C*),

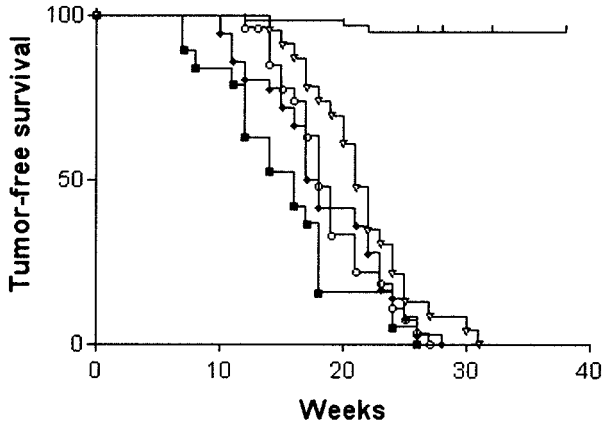

Fig. 1. Tumor-free survival of mice of different genotypes. Mice were sacrificed when they became moribund. ■, *Ink4d*$^{+/+}$, *Ink4c*$^{+/+}$, *p53*$^{-/-}$ (n = 19); ▽, *Ink4d*$^{+/+}$, *Ink4c*$^{+/-}$, *p53*$^{-/-}$ (n = 23); ◆, *Ink4d*$^{+/+}$, *Ink4c*$^{-/-}$, *p53*$^{-/-}$ (n = 36); ○, *Ink4d*$^{-/-}$, *Ink4c*$^{-/-}$, *p53*$^{-/-}$ (n = 27); (⊥) *Ink4d*$^{+/+}$, *Ink4c*$^{-/-}$, *Arf*$^{-/-}$ (n = 62).

Table 1 *Incidence of tumors in p53-null mice lacking different Ink4 alleles*

Genotype	Mean age (wks)	Vascular tumors and dysplasias	Brain tumors	Pituitary adenoma	Lymphoma (B and T cell)	Others[a]
$Ink4d^{+/+}Ink4c^{+/+}$, $n = 19$	15.4	13 (68%)	1 (5%)	0 (0%)	14 (74%)	3 (16%)
$Ink4d^{+/+}Ink4c^{+/-}$, $n = 23$	21.5	19 (83%)	0 (0%)	0 (0%)	13 (57%)	3 (13%)
$Ink4d^{+/+}Ink4c^{-/-}$, $n = 36$	18.4	32 (89%)	3 (8%)	8 (22%)	18 (50%)	8 (22%)
$Ink4d^{+/-}Ink4c^{+/-}$, $n = 13$	17.7	11 (85%)	2 (15%)	0 (0%)	8 (62%)	2 (15%)
$Ink4d^{+/-}Ink4c^{-/-}$, $n = 38$	18.4	34 (89%)	9 (24%)	12 (32%)	24 (63%)	4 (11%)
$Ink4d^{-/-}Ink4c^{+/+}$, $n = 10$	17.1	7 (70%)	1 (10%)	0 (0%)	6 (60%)	4 (40%)
$Ink4d^{-/-}Ink4c^{+/-}$, $n = 17$	20.3	14 (82%)	1 (6%)	1 (6%)	11 (65%)	3 (18%)
$Ink4d^{-/-}Ink4c^{-/-}$, $n = 27$	18.9	23 (85%)	0 (0%)	11 (41%)	19 (70%)	5 (19%)

[a] A broad spectrum of tumor types was detected at relatively low frequencies. In many cases, multiple tumors arising from different tissue types appeared in individual animals. These included nonvascular sarcomas (leiomyosarcoma, rhabdomyosarcoma, and osteogenic, histiocytic, pleomorphic, and epithelioid sarcomas; total = 10 tumors), various carcinomas (squamous cell, intestinal, and pancreatic adenocarcinoma; total = 11 tumors), benign tumors (adenomas, papillomas, lipoma, and nerve sheath tumor; total = 4 tumors); and testicular tumors also seen in *p53*-null (teratomas) and *Ink4c*-null mice (Leydig cell tumors; total = 10 tumors).

CD34 (Fig. 2*D*), VEGF-R2 (Fig. 2*E*), and von Willebrand factor (Factor 8; data not shown). The incidence of hemangiosarcomas was high in all *p53*-null mice lacking at least one *Ink4c* allele (Table 2).

Because many vascular tumors were aggressive, we transplanted several hemangiosarcomas from mice of different founding genotypes into immunocompromised NOD/SCID recipients. Primary tumors (Fig. 2, *F* and *G*) were excised and divided, and pieces were injected s.c. into cohorts of three to six recipient animals. As a positive control, we used a transformed endothelial cell line, EOMA, which is vascular endothelial growth factor independent, can form capillaries when grown in Matrigel, and can be easily propagated by transplantation. Many of the primary tumors could be transplanted, reappearing and growing at s.c. sites of implantation within a month in at least some recipients (Fig. 2*H*). These transplanted tumors exhibited the same pathological characteristics as those seen in the primary tumors from $Ink4c^{+/-}/p53^{-/-}$ or $Ink4c^{-/-}/p53^{-/-}$ animals and were virtually indistinguishable from them (Fig. 2, *H* and *I*). These tumors can now be serially transplanted. To date, however, all attempts to propagate primary hemangiosarcomas in tissue culture have been unsuccessful, possibly because the tumors consist of multiple cell populations, of which endothelial cells represent only one component.

Medulloblastomas Develop in Mice Lacking *Ink4c* and *p53* but Retaining *Ink4d*. Unexpectedly, mice lacking *p53* and *Ink4c*, but retaining one or two copies of *Ink4d*, developed brain tumors in addition to all other tumors listed in Table 1. The frequency of brain tumor formation ranged from 8% to 24% in animals lacking *Ink4c* alleles (Table 1) but dropped to 3.7% in mice also lacking both *Ink4d* alleles. The latter differences were significant ($P < 0.02$), implying that complete *Ink4d* loss counteracts these effects of *Ink4c* deletion. Moreover, whereas *Ink4c* loss predisposes animals to medulloblastoma formation (see below), the two brain tumors detected in animals lacking *p53* and *Ink4d* but retaining one or both copies of *Ink4c* represented rare PNETs, perhaps reflecting only *p53* deficiency, as described earlier by others (26). The similar frequency of tumor formation in *Ink4c* heterozygotes and *Ink4c*-null mice could reflect inactivation of the wild-type allele or haploinsufficiency at the *Ink4c* locus, which has been demonstrated in other settings (28). This has not been further studied.

Brain tumors in the *Ink4c/p53*-deficient animals, 15 *in toto*, included a majority (12) that were predominantly cerebellar (Table 3). The tumors tended to spread along the surface of the cerebellar cortex and often grew outward as exophytic masses. Inward infiltration of the tumor through the molecular layer and into the granular cell layer and cerebellar white matter was also observed in the majority of cases (Fig. 3*A*). In one mouse, the cerebellar tumor extended into the brain stem; in another, separate tumor foci were seen in the olfactory bulb. Cerebellar tumors exhibited closely packed, round to oval embryonal cells with scant cytoplasm (Fig. 3*B*) that closely resembled human medulloblastomas (Fig. 3*C*). The tumors often contained anaplastic regions with enlarged cells, cellular wrapping, and increased mitotic activity (Fig. 3*D*), features commonly found in human anaplastic medulloblastoma. Tumor nodules in the brain stem (Fig. 3*E*) and cerebral cortex (Fig. 3*F*) were also densely cellular and contained cells with prominent nucleoli and tumor giant cells. To confirm that the cerebellar tumors were medulloblastomas and not other primary central nervous system neoplasms or metastatic lesions, such as lymphomas, sections were stained for markers of glial (GFAP; Fig. 3*G*) and neuronal (synaptophysin; Fig. 3*H*) differentiation and for the intermediate filament nestin (Fig. 3*I*), which is expressed in primitive neuroepithelial cells and embryonal tumors. All cerebellar tumors

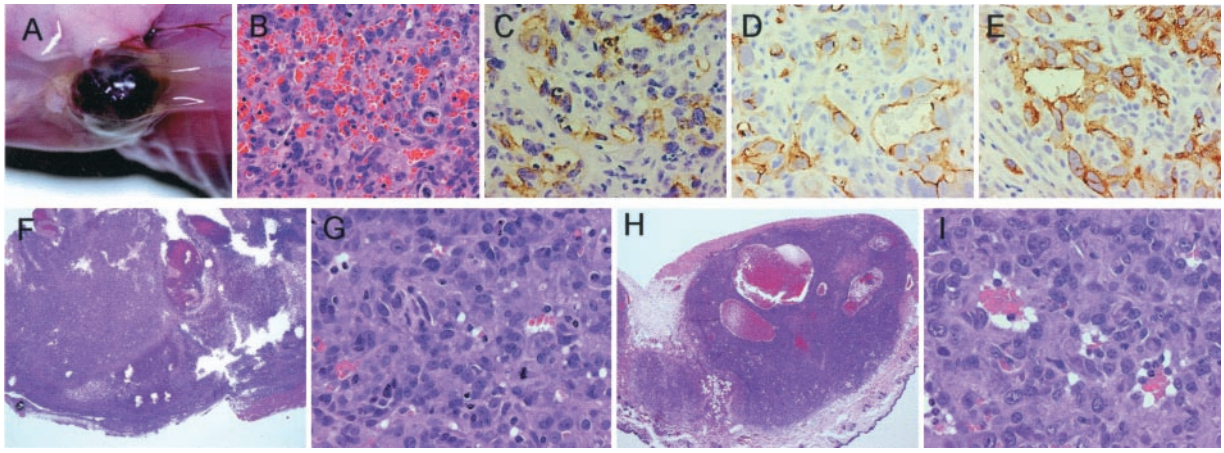

Fig. 2. Hemangiosarcomas in *p53/Ink4c*-null mice. *A*, a representative tumor invading skeletal muscle. *B*, tumor histology, H&E stain. *C–E*, immunohistochemical staining for CD31 (*C*), CD34 (*D*), and VEGF-R2 (*E*). *F*, a primary tumor taken for transplantation with tumor histology shown in *G*. *H*, a transplanted tumor arising in a NOD/SCID mouse, with tumor histology shown in *I*.

Table 2 *Incidence of hemangiosarcomas in p53-null mice lacking Ink4 alleles*

Genotype	Hemangiosarcoma incidence[a]
$Ink4d^{+/+}Ink4c^{+/+}$	9/19 (47%)
$Ink4d^{+/+}Ink4c^{+/-}$	17/23 (74%)
$Ink4d^{+/+}Ink4c^{-/-}$	26/36 (72%)
$Ink4d^{+/-}Ink4c^{+/-}$	11/13 (85%)
$Ink4d^{+/-}Ink4c^{-/-}$	26/38 (68%)
$Ink4d^{-/-}Ink4c^{+/+}$	5/10 (50%)
$Ink4d^{-/-}Ink4c^{+/-}$	13/17 (76%)
$Ink4d^{-/-}Ink4c^{-/-}$	17/27 (63%)

[a] Number of affected animals versus total number analyzed in cohorts of the indicated genotypes.

stained positively for each of these markers in areas with little or no normal brain tissue, confirming that they exhibited divergent neuroectodermal differentiation and were *bona fide* medulloblastomas.

Tumors involving only the cerebral cortex or brain stem were also densely cellular and were somewhat more infiltrative than the cerebellar medulloblastomas. However, like the medulloblastomas, these extracerebellar lesions were also made up of highly atypical cells expressing GFAP, synaptophysin, and nestin. The WHO classification designates embryonal lesions with divergent differentiation arising outside the cerebellum as PNET, and we classified the murine extracerebellar tumors according to this scheme.

Examination of more than 30 cerebella from brain tumor-free animals of similar genotypes and ages (4–5 months) as the ones that developed medulloblastoma failed to reveal definitive precursor lesions. However, in several cases with smaller cerebellar lesions, the bulk of the tumor was clearly on the surface of the brain with only limited inward growth, suggesting that the tumors might arise at peripheral sites occupied by the proliferating EGL during cerebellar development. Brain stem lesions located adjacent to the fourth ventricle could have arisen from periventricular germinal matrix cells. An expanded and cytologically atypical ventricular zone subadjacent to the lateral ventricle in one mouse lacking an overt tumor could represent a precursor of supratentorial PNET. In animals with both cerebellar and cortical tumors, the cortical lesions could either have arisen independently or spread from the primary cerebellar site via the cerebral spinal fluid, as often occurs in humans.

To further assess the different contributions of *Ink4c* and *Ink4d* to tumor development, we evaluated their expression by *in situ* RNA hybridization in the cerebella of wild-type mice from E11.5 into adulthood (Fig. 4). At E11.5 (Fig. 4, *A* and *K*), the cerebellar anlage is a crescent-shaped structure consisting of a thick NE containing dividing neuroblasts and a DZ containing the earliest developing nuclear cells. At this time, an epithelial layer that covers the cerebellum will develop into the pial membrane (*pia*). Another epithelial layer, the medullary vellum (*mv*), will develop into the roof of the fourth ventricle. Expression of *Ink4c* RNA was detected in the developing pia (Fig. 4*B*), whereas *Ink4d* RNA was localized to the DZ (Fig. 4*L*). No expression of either gene was seen within the NE. By E13.5 (Fig. 4, *C* and *M*), the cerebellar anlage becomes a closed outpocketing of the hindbrain containing three distinct DZs. Recently born nuclear cells produced in the NE reside in DZ1 and move to their final position in DZ2, whereas early postmitotic Purkinje cells reside in DZ3. *Ink4c* and *Ink4d* were expressed in the pia (Fig. 4*D*) and in DZ1 and DZ3 (Fig. 4*N*), respectively.

By E15.5, cells from the posterolateral GT (Fig. 4*P*) have migrated along the cerebellar surface to form the developing EGL, below which is a 3–4-cell-thick plate of Purkinje cells (PCPs; Fig. 4, *E* and *P*). *Ink4c* was expressed in the pial membrane and in ossifying chondrocytes of the developing skull (Fig. 4*F*), and an increased intensity of *Ink4d* staining marked the PCPs (Fig. 4*P*). Importantly, at this time, cells in the GT and within the EGL do not express *Ink4* RNAs. However, during the first 2 postnatal weeks of life, granule cells rapidly proliferate, leave the EGL, and migrate to form the IGL. At P5 (Fig. 4, *G* and *Q*), the cerebellar cortex, covered by the thickened *Ink4c*-expressing pia (Fig. 4*H*), consists of four layers: the rapidly proliferating granule cells of the EGL; an underlying molecular layer; a multilaminar PCP; and the nascent IGL. At this time, *Ink4c* expression was detected within the proliferative zone of the EGL. Other markers of proliferating GCPs, including the Math1 transcription factor and Ki67, are also expressed in this population, whereas *Kip1* expression is confined to a deeper layer of cells that have exited the cell division cycle and to Purkinje cells (data not shown). *Ink4d* was expressed in Purkinje cells and in deeper cerebellar nuclear cells (Fig. 4*R*). Hence, *Ink4c*, but not *Ink4d*, is expressed at P5 in GCPs that are presumed to give rise to medulloblastomas (29).

In the adult cerebellum (Fig. 4, *I* and *S*), all cells formerly in the EGL have migrated to the IGL, so that a trilaminar cortex is established containing an outer molecular layer, a single layer of Purkinje cells (Fig. 4*S*, *pcl*), and the IGL. High levels of *Ink4c* expression persisted only in the pial layer (Fig. 4*J*), whereas *Ink4d* expression was maintained in Purkinje cells and in deeper cerebellar nuclear cells (Fig. 4*T*).

Table 3 *Incidence, location, and type of brain tumors in p53-null mice lacking Ink4 alleles*

Six cohorts of mice developed brain tumors (Table 1). No animals lacking both *Ink4d* alleles developed medulloblastomas, but these animals died of other tumor types at the same mean age as other cohorts (Fig. 1).

Genotype	Incidence	Age (wks)	Tumor sites	Tumor histology
$Ink4d^{+/+}Ink4c^{+/+}$	1/19 (5%)	24	Brain stem	PNET
$Ink4d^{+/+}Ink4c^{+/-}$	0/23 (0%)	22	None	
$Ink4d^{+/+}Ink4c^{-/-}$	3/36 (8%)	12	Cerebellum	MB[a]
		16	Posterior cerebellum	MB
		17	Dorsal cerebellum	MB with moderate anaplasia
$Ink4d^{+/-}Ink4c^{+/-}$	2/13 (15%)	19	Cerebellum/brainstem	MB with moderate anaplasia
		26	Ventral posterior cerebellum and PVZ[b]/thalamus	MB/PNET
$Ink4d^{+/-}Ink4c^{-/-}$	9/38 (24%)	13	Brain stem	PNET
		16	Dorsal cerebellum	MB with moderate anaplasia
		17	Cerebellum	MB
		19	Cerebellum	MB with moderate anaplasia
		20	Cerebellum	MB
		20	Cerebellum and olfactory bulb	MB with severe anaplasia/PNET
		22	Dorsal cerebellum	MB with moderate anaplasia
		24	Ventral brain stem/base of brain	PNET
		28	Dorsal cerebellum	MB with severe anaplasia
$Ink4d^{-/-}Ink4c^{+/+}$	1/10 (10%)	12	Cerebrum	PNET
$Ink4d^{-/-}Ink4c^{+/-}$	1/17 (6%)	23	Brain stem	PNET
$Ink4d^{-/-}Ink4c^{-/-}$	0/27 (0%)	19	None	

[a] MB, medulloblastoma; [b] PVZ, periventricular zone.

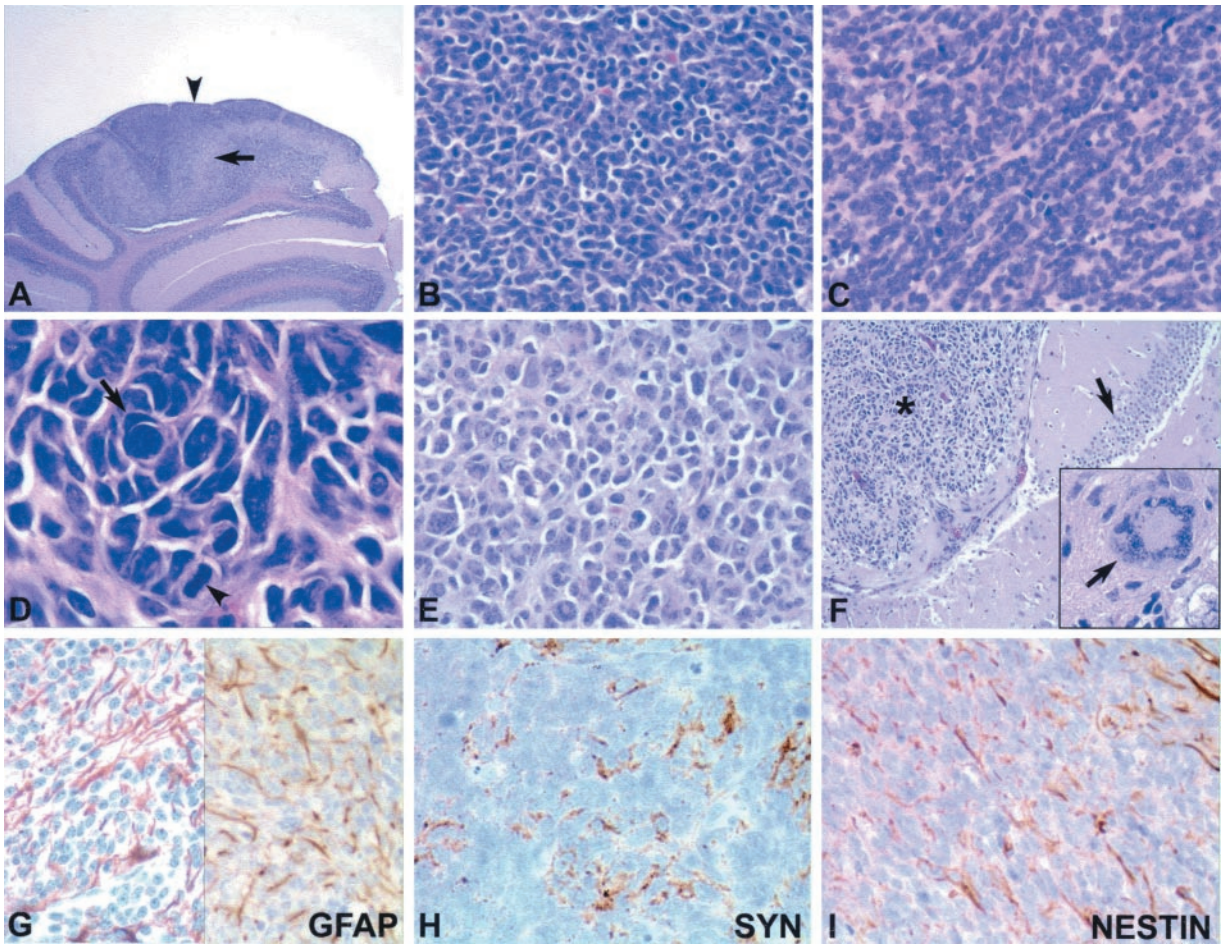

Fig. 3. Histopathology of brain tumors. *A,* tumors arising in *Ink4c/p53*-null mice were most often centered on the cerebellar surface (*arrowhead*) and invaded inward through the molecular layer into the IGL (*arrow*; ×200 magnification). *B,* tumors were composed of closely packed embryonal cells with little cytoplasm (×400). *C,* human medulloblastoma (×400). *D,* murine medulloblastomas often contained anaplastic regions with enlarged cells, cellular wrapping (*arrow*), and increased mitotic activity (*arrowhead*; ×1000). *E,* brain stem lesion containing enlarged tumor cells with prominent nucleoli (×400). *F,* tumor nodules detected at supratentorial sites remote from the cerebellar lesion, such as a cortical lesion (*asterisk*) adjacent to the hippocampus (*arrow*; ×100). Giant cells were identified in some cerebral lesions (*inset*). *G,* like human medulloblastoma (*left panel*), many mouse tumors showed glial differentiation as evidenced by GFAP expression (*right panel,* ×400). *H,* scattered synaptophysin-positive cells were also present in the same lesions (×400). *I,* nestin, a marker of primitive neuroepithelial cells, was also expressed in tumor cell processes.

DISCUSSION

Collaboration between *Ink4c* and *p53*, but not *Arf*. Cohorts of mice with combined loss of *Ink4c* and *p53*, regardless of *Ink4d* status, exhibited a broader spectrum of tumors than those observed in parental *p53*-null and *Ink4c*-null strains. Of particular interest was the high incidence of hemangiosarcomas and the appearance of medulloblastomas, the latter not previously observed in the parental strains. Mice lacking *Ink4c* and *p53* were so tumor-prone that necropsy of moribund animals usually revealed multiple primary tumors per animal, which frequently arose from entirely different cell types. Interestingly, no synergy was observed between *Ink4c* and *Arf* loss, at least during the relatively short postnatal period in which *Ink4c/p53*-null mice developed tumors and died. Despite the fact that $p19^{Arf}$ activates p53 in response to abnormally amplified mitogenic signals (30), *Arf* is actively repressed during embryonic mouse development (31), and its expression is muted in young healthy mice (9). Moreover, p53 responds to a much broader spectrum of stress signal inputs than does *Arf*, particularly those triggered by genotoxic damage. Thus, the events that lead to the formation of vascular and brain tumors in *Ink4c/p53*-null mice might occur during early development when *Arf* is silent and result as a consequence of replicative DNA damage in the absence of appropriate p53 checkpoint control.

Vascular Tumorigenesis at High Penetrance. Animals lacking both *p53* and *Ink4c* presented with vascular tumors, the majority of which were invasive. Mice lacking *p53* and *Ink4a* also develop such tumors with a high (56%) incidence (32), and it remains unclear whether loss of *Ink4c* has more profound effects than *Ink4a* in this regard, or whether the observed frequencies simply reflect strain differences. $Ink4c^{+/-}/p53^{-/-}$ mice also developed hemangiosarcomas, but analysis of loss of heterozygosity in these tumors was not possible, due to the mixture of cell types that comprise the tumors and the ambiguity of which cell type (endothelial or mesenchymal) is the actual tumor cell. However, haploinsufficiency for tumor formation was recently revealed when $Ink4c^{+/-}$ mice were challenged with chemical carcinogens (28).

Primary hemangiosarcomas were serially transplantable by dividing tumors into pieces and introducing them s.c. into cohorts of immunocompromised mice. Not every animal receiving portions of the same primary tumor initially developed a secondary tumor at the injection site. Moreover, we were unable to establish tumor cell lines when we explanted primary tumors into culture. We therefore suspect that these tumors may be composed of interacting cell types that must be propagated in such a way that appropriate cell-cell interactions are maintained. In short, although the endothelial component of these

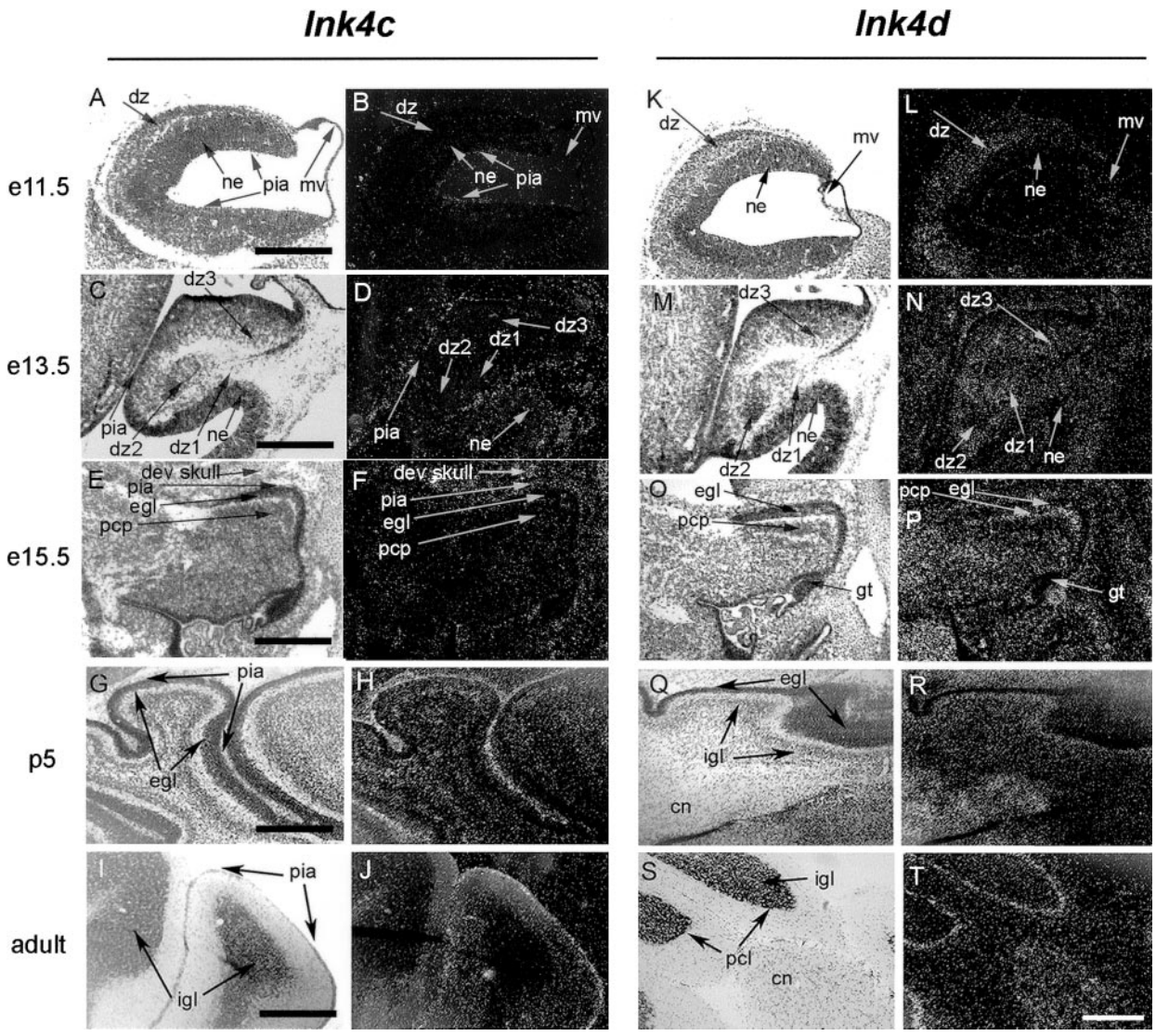

Fig. 4. *In situ* expression of *Ink4c* and *Ink4d* mRNAs in the developing cerebellum (from E11.5 to P5) and in the adult brain. The formation of the cerebellum from E11.5 through the first postnatal weeks of life is described in the text. It is thought that rapidly proliferating GCPs that make up the EGL of the developing cerebellum can sustain oncogenic insults that lead to formation of medulloblastomas. *cn*, cerebellar nucleus; *dev skull*, developing skull; *dz*, DZ; *egl*, EGL; *gt*, GT; *mv*, medullary vellum; *ne*, neuroepithelium; *pcl*, Purkinje cell layer; *pcp*, PCPs; *pia*, pia mater; *igl*, IGL. *Scale bars*: *A, B, K,* and *L,* 100 μm; *C, D, M,* and *N,* 150 μm; *E, F, O,* and *P,* 200 μm; *G, H, I* and *R,* 200 μm; *I, J, S,* and *T,* 200 μm.

tumors is prominent, there is no direct evidence that the proliferation of endothelial cells results from their oncogenic transformation, as opposed to their mitogenic stimulation by neighboring cells.

Roles of *Ink4c* and *Ink4d* in Medulloblastoma Formation. Medulloblastomas, which are cerebellar embryonal neoplasms, do not arise in *Ink4c*-null or *p53*-null mice, but they appeared at a significant frequency in animals lacking both genes. Analysis of tumor histology, histochemistry, and patterns of invasion and metastasis revealed that these tumors shared many of the hallmarks of human anaplastic medulloblastomas. Medulloblastomas represent the most common malignant brain tumor in children and remain difficult to treat by combined surgical, chemo-, and radiotherapy (5-year survival, ~50%). Similar lesions, known as PNETs, which can arise outside of the posterior fossa, albeit rarely, have been observed infrequently in *p53*-null animals (26).

During late embryogenesis, neural precursor cells migrate from a dorsal hindbrain structure, the rhombic lip, and advance along the cerebellar surface to form the EGL, which, in mice at birth, consists of only a single layer of cells. Postnatally, this population rapidly expands to generate a large pool of GCPs. Much of this expansion is regulated by diffusible factors, which, among others, include Shh released by neighboring Purkinje cells, Notch and Wnt ligands released by GCPs themselves, and the chemokine SDF-1α, which is released by pial cells on the cerebellar surface (29, 33–35). Once expanded, GCPs exit the EGL, migrating through the Purkinje cell layer to form the IGL and maturing into granule neurons by the third postnatal week. By the time this process is completed, the major population of neurons in the entire adult brain comes to consist of cerebellar granule cells.

Most investigators believe that medulloblastomas arise from GCPs that sustain mutations and are unable to properly differentiate (29). Consistent with this view, about 30% of human medulloblastomas sustain mutations in the Shh signaling pathway that involve genes such as Patched (*Ptc1*), Smoothened (*Smo*), and Suppressor of Fused (*SuFu*), leading to constitutive activation of Gli transcription factors (29, 33). Shh signaling also up-regulates the c- and N-*Myc* genes, which are amplified in 10% of medulloblastomas and highly expressed in many more (36, 37). *Ptc1*$^{+/-}$ mice develop medulloblastomas (29), and the incidence of tumors approaches 100% on a *p53*-null background (although, here again, loss of *Arf* does not

accelerate disease; Ref. 38). Animals lacking *ligase IV* die *in utero* but are rescued on a *p53*-null background (39); these mice also develop medulloblastomas, implying that DNA damage in the absence of p53 checkpoint control can initiate such tumors (40). *p53* and *Rb* loss can collaborate in this setting because their targeted codeletion in the cerebellum results in medulloblastomas with full penetrance (41). In principle, *Ink4c* loss might mimic the effects of *Rb* loss and similarly contribute.

Oligonucleotide microchip arrays performed with RNAs taken from medulloblastomas arising in mice of different genotypes (including $Ptc1^{+/-}/p53^{-/-}$, $LigIV^{-/-}/p53^{-/-}$, and $Ink4c^{-/-}/p53^{-/-}$) compared with RNA from the cerebellum of normal 5-day-old mice revealed that the medulloblastomas exhibited strikingly similar patterns of gene expression. Many tumors overexpressed *Gli1*, N-*Myc*, c-*Myc*, *cyclin D1*, and the SDF-1α receptor *CXCR4* by at least 5-fold (42). Therefore, they appeared to exhibit up-regulated Shh signaling, despite the different founding mutations that initiated tumorigenesis.

Ink4c expression was restricted to the developing postnatal EGL and otherwise was mostly confined to pial cells. We suspect that expression of $p18^{Ink4c}$ in GCPs acts together with $p27^{Kip1}$ to regulate mitotic exit, after which only $p27^{Kip1}$ expression is maintained in the postmitotic granule neurons that migrate from the EGL into the IGL. The brains of either *Ink4c*-null or *Kip1*-null mice are enlarged and contain extra neurons, but these cells seem to differentiate and migrate properly and make appropriate connections to other cerebellar neurons because no overt neurological deficits are observed in such mice (14–19). Although loss of *Kip1* leads to increased proliferation in many parts of the brain, especially in regions of continuous proliferation such as the dentate gyrus, this is insufficient to induce brain tumors. Brain tumors have not been reported in any other mouse cohorts where *Cip*/*Kip* genes were deleted alone, in combination, or with *p53*. Therefore, defects in cell cycle regulation *per se* may not account for medulloblastoma development in *Ink4c*/*p53*-null mice.

Knoepfler and collaborators (43) recently found that *Ink4c* and *Kip1* are highly expressed in the embryonic cerebellar primordium of mice in which N-*Myc* was conditionally deleted using a *Nestin-Cre* transgene. These mice develop a small cerebellum, presumably due to the abnormal expression of CKIs that suppress proliferation of the EGL. Hence, *Ink4c* and *Kip1* are down-regulated by N-*Myc*, and this is likely necessary for proper granule cell development.

Ink4d was expressed in postmitotic Purkinje neurons, and its loss countered the development of medulloblastomas. Because these tumors are presumed to arise from GCPs, loss of *Ink4c* and *Ink4d* might affect the release of diffusible factors from pial and Purkinje cells, respectively, that sandwich the developing EGL. Because we saw no overt expansion of pial and Purkinje populations, there is no evidence that the role of the Ink4 proteins is to regulate their cell cycles. Instead, it may prove that the Ink4 proteins govern Rb family-dependent transcriptional programs that control cell-cell communication and the subsequent expansion and differentiation of GCPs. Evaluation of the levels of regulatory factors, such as Shh and SDF-1α, produced by Purkinje and pial cells from *Ink4*-deficient animals should improve our understanding of the processes involved.

ACKNOWLEDGMENTS

We thank Patricia Jensen and Susan Magdaleno for assistance with *in situ* RNA hybridization; Adriana Nance, Linda Horner, Brenda McGowan, and Kellie Ann Christie for preparing mouse tissues for histopathology; Linda Sharp and Eduardo Vasquez for handling mouse colonies; Dorothy Bush for immunostaining; Guylaine Assem, Camu Pous Hornsby, Sussy Portillo, and Rema Menon for mouse genotyping; Jeremy D. Creech and Peter Houghton for tumor transplants; and Chenghong Li and Xiaoping Xiong for statistical analysis.

REFERENCES

1. Sherr, C. J., and Roberts, J. M. Inhibitors of mammalian G_1 cyclin-dependent kinases. Genes Dev., *9:* 1149–1163, 1995.
2. Harper, J. W., and Elledge, S. J. Cdk inhibitors in development and cancer. Curr. Opin. Genet. Dev., *6:* 56–64, 1996.
3. Nakayama, K., and Nakayama, K. Cip/Kip cyclin-dependent kinase inhibitors: brakes of the cell cycle engine during development. Bioessays, *20:* 1020–1029, 1998.
4. Ortega, S., Malumbres, M., and Barbacid, M. Cyclin D-dependent kinases, INK4 inhibitors and cancer. Biochim. Biophys. Acta, *1602:* 73–87, 2002.
5. Dyson, N. The regulation of E2F by pRB-family proteins. Genes Dev., *12:* 2245–2262, 1998.
6. Nevins, J. R. The Rb/E2F pathway and cancer. Hum. Mol. Genet., *10:* 699–703, 2001.
7. Trimarchi, J. M., and Lees, J. A. Sibling rivalry in the E2F family. Nat. Rev. Mol. Cell. Biol., *3:* 11–20, 2002.
8. Sherr, C. J., and Roberts, J. M. CDK inhibitors: positive and negative regulators of G_1-phase progression. Genes Dev., *13:* 1501–1512, 1999.
9. Zindy, F., Quelle, D. E., Roussel, M. F., and Sherr, C. J. Expression of the $p16^{INK4a}$ tumor suppressor *versus* other INK4 family members during mouse development and aging. Oncogene, *15:* 203–211, 1997.
10. Zindy, F., Soares, H., Herzog, K-H., Morgan, J., Sherr, C. J., and Roussel, M. F. Expression of INK4 inhibitors in cyclin D-dependent kinases during mouse brain development. Cell Growth Differ., *8:* 1139–1150, 1997.
11. Zindy, F., Cunningham, J. J., Sherr, C. J., Jogal, S., Smeyne, R. J., and Roussel, M. F. Postnatal neuronal proliferation in mice lacking Ink4d and Kip1 inhibitors of cyclin-dependent kinases. Proc. Natl. Acad. Sci. USA, *96:* 13462–13467, 1999.
12. Lowenheim, H., Furness, D. N., Kil, J., Zinn, C., Gultig, K., Fero, M. L., Frost, D., Gummer, A. W., Roberts, J. M., Rubel, E. W., Hackney, C. M., and Zenner, H-P. Gene disruption of $p27^{Kip1}$ allows cell proliferation in the postnatal and adult organ of Corti. Neurobiology, *96:* 4084–4088, 1999.
13. Chen, P., Zindy, F., Abdala, C., Liu, F., Li, X., Roussel, M. F., and Segil, N. Progressive hearing loss in mice lacking the cyclin-dependent kinase inhibitor *Ink4d*. Nat. Cell Biol., *5:* 422–426, 2003.
14. Fero, M. L., Rivkin, M., Tasch, M., Porter, P., Carow, C. E., Firpo, E., Polyak, K., Tsai, L-H., Broudy, V., Perlmutter, R. M., Kaushansky, K., and Roberts, J. M. A syndrome of multiorgan hyperplasia with features of gigantism, tumorigenesis, and female sterility in $p27^{Kip1}$-deficient mice. Cell, *85:* 733–744, 1996.
15. Kiyokawa, H., Kineman, R. D., Manova-Todorova, K. O., Soares, V. C., Hoffman, E. S., Ono, M., Khanam, D., Hayday, A. C., Frohman, L. A., and Koff, A. Enhanced growth of mice lacking the cyclin-dependent kinase inhibitor function of $p27^{Kip1}$. Cell, *85:* 721–732, 1996.
16. Nakayama, K., Ishida, N., Shirane, M., Inomata, A., Inoue, T., Shishido, N., Horii, I., and Loh, D. Y. Mice lacking $p27^{Kip1}$ display increased body size, multiple organ hyperplasia, retinal dysplasia, and pituitary tumors. Cell, *85:* 707–720, 1996.
17. Franklin, D. S., Godfrey, V. L., Lee, H., Kovalev, G. I., Schoonhoven, R., Chen-Kiang, S., Su, L., and Xiong, Y. CDK inhibitors $p18^{Ink4c}$ and $p27^{Kip1}$ mediate two separate pathways to collaboratively suppress pituitary tumorigenesis. Genes Dev., *12:* 2899–2911, 1998.
18. Latres, E., Malumbres, M., Sotillo, R., Martin, J., Ortega, S., Martin-Caballero, J., Flores, J. M., Cordon-Cardo, C., and Barbacid, M. Limited overlapping roles of $P15^{INK4b}$ and $P18^{INK4c}$ cell cycle inhibitors in proliferation and tumorigenesis. EMBO J., *19:* 3496–3506, 2000.
19. Franklin, D. S., Godfrey, V. L., O'Brien, D. A., Deng, C., and Xiong, Y. Functional collaboration between different cyclin-dependent kinase inhibitors suppresses tumor growth with distinct tissue specificity. Mol. Cell. Biol., *20:* 6147–6158, 2000.
20. Zindy, F., den Besten, W., Chen, B., Rehg, J. E., Latres, E., Barbacid, M., Pollard, J. W., Sherr, C. J., Cohen, P. E., and Roussel, M. F. Control of spermatogenesis in mice by the cyclin D-dependent kinase inhibitors $p18^{Ink4c}$ and $p19^{Ink4d}$. Mol. Cell. Biol., *21:* 3244–3255, 2001.
21. Jacks, T., Remington, L., Williams, B. O., Schmitt, E. M., Halachmi, S., Bronson, R. T., and Weinberg, R. A. Tumor spectrum analysis in p53-mutant mice. Curr. Biol., *4:* 1–7, 1994.
22. Obeso, J., Weber, J., and Auerback, R. A hemangioendothelioma-derived cell line: its use as a model for the study of endothelial cell biology. Lab. Investig., *63:* 259–269, 1990.
23. Leggas, M., Stewart, C. F., Woo, M. H., Fouladi, M., Cheshire, P. J., Peterson, J. K., Friedman, H. S., Billups, C., and Houghton, P. J. Relation between Irofulven (MGI-114) systemic exposure and tumor response in human solid tumor xenografts. Clin. Cancer Res., *8:* 3000–3007, 2002.
24. Cerilli, L. A., and Wick, M. R. Immunohistology of soft tissue and osseous neoplasms. *In:* D. J. Dabbs (ed.), Diagnostic Immunohistochemistry, pp. 59–112. New York: Churchill Livingstone (Harcourt Health Sciences), 2002.
25. Inoue, K., Wren, R., Rehg, J. E., Adachi, M., Cleveland, J. L., Roussel, M. F., and Sherr, C. J. Disruption of the *ARF* transcriptional activator *DMP1* facilitates cell immortalization, Ras transformation, and tumorigenesis. Genes Dev., *14:* 1797–1809, 2000.
26. Donehower, L. A., Harvey, M., Slagle, B. L., McArthur, M. J., Montgomery, C. A., Jr., Butel, J. S., and Bradley, A. Mice deficient for p53 are developmentally normal but susceptible to spontaneous tumours. Nature (Lond.), *356:* 215–221, 1992.
27. Donehower, L. A., Harvey, M., Vogel, H., McArthur, M. J., Montgomery, C. A., Jr., Park, S. H., Thompson, T., Ford, R. J., and Bradley, A. Effects of genetic background on tumorigenesis in *p53*-deficient mice. Mol. Carcinog., *14:* 16–22, 1995.
28. Bai, F., Pei, X. H., Godfrey, V. L., and Xiong, Y. Haploinsufficiency of $p18^{INK4c}$ sensitizes mice to carcinogen-induced tumorigenesis. Mol. Cell. Biol., *23:* 1269–1277, 2003.

29. Wechsler-Reya, R. J., and Scott, M. P. The developmental biology of brain tumors. Annu. Rev. Neurosci., *24:* 385–428, 2001.
30. Sherr, C. J. The. INK4a/ARF network in tumour suppression. Nat. Rev. Mol. Cell. Biol., *2:* 731–737, 2001.
31. Jacobs, J. J. L., Kieboom, K., Marino, S., DePinho, R. A., and van Lohuizen, M. The oncogene and Polycomb-group gene *bmi-1* regulates cell proliferation and senescence through the *ink4a* locus. Nature (Lond.), *397:* 164–168, 1999.
32. Sharpless, N. E., Alson, S., Chan, S., Silver, D. P., Castrillon, D. H., and DePinho, R. A. $p16^{INK4a}$ and p53 deficiency cooperate in tumorigenesis. Cancer Res., *62:* 2761–2765, 2002.
33. Rubin, J. B., and Rowitch, D. H. Medulloblastoma: a problem of developmental biology. Cancer Cell, *2:* 7–8, 2002.
34. Klein, R. S., Rubin, J. B., Gibson, H. D., DeHaan, E. N., Alvarez-Hernandez, X., Segal, R. A., and Luster, A. D. SDF-1a induces chemotaxis and enhances Sonic hedgehog-induced proliferation of cerebellar granule cells. Development (Camb.), *128:* 1971–1981, 2001.
35. Zhu, Y., Yu, T., Zhang, X-C., Nagasawa, T., Wu, J. Y., and Rao, Y. Role of the chemokine SDF-1 as the meningeal attractant for embryonic cerebellar neurons. Nat. Neurosci., *5:* 719–720, 2002.
36. Kenney, A. M., Cole, M. D., and Rowitch, D. H. N-myc upregulation by sonic hedgehog signaling promotes proliferation in developing cerebellar granule neurons. Development (Camb.), *130:* 15–28, 2003.
37. Berman, D. M., Karhadkar, S. S., Hallahan, A. R., Pritchard, J. I., Eberhart, C. G., Watkins, D. N., Chen, J. K., Cooper, M. K., Taipale, J., Olson, J. M., and Beachy, P. A. Medulloblastoma growth inhibition by hedgehog pathway blockade. Science (Wash. DC), *297:* 1559–1561, 2002.
38. Wetmore, C., Eberhart, D. E., and Curran, T. Loss of *p53* but not *ARF* accelerates medulloblastoma in mice heterozygous for *patched.* Cancer Res., *61:* 513–516, 2001.
39. Frank, K. M., Sharpless, N. E., Gao, Y., Sekiguchi, J. M., Ferguson, D. O., Zhu, C., Manis, J. P., Horner, J., DePinho, R. A., and Alt, F. W. DNA ligase IV deficiency in mice leads to defective neurogenesis and embryonic lethality via the p53 pathway. Mol. Cell, *5:* 993–1002, 2000.
40. Lee, Y., and McKinnon, P. J. DNA ligase IV suppresses medulloblastoma formation. Cancer Res., *62:* 6395–6399, 2002.
41. Marino, S., Vooijs, M., van der Gulden, H., Jonkers, J., and Berns, A. Induction of medulloblastomas in *p53*-null mutant mice by somatic inactivation of *Rb* in the external granular layer cells of the cerebellum. Genes Dev., *14:* 994–1004, 2000.
42. Lee, Y., Miller, H. L, Jensen, Pl, Hernan, R., Connelly, M., Wetmore, C., Zindy, F., Roussel, M., Curran, T., Gilbertson, R., and McKinnon, P. J. A molecular fingerprint for medulloblastoma. Cancer Res., *63:* 5427–5436, 2003.
43. Knoepfler, P. S., Cheng, P. F., and Eisenman, R. N. N-*myc* is essential during neurogenesis for the rapid expansion of progenitor cell populations and the inhibition of neuronal differentiation. Genes Dev., *16:* 2699–2712, 2002.